Aalborg Universitet

Three-Phase Grid-Connected of Photovoltaic Generator Using Nonlinear Control

Yahya, A.; El Fadil, H.; Guerrero, Josep M.; Giri, F.; Erguig, H.

Three-Phase Grid-Connected of Photovoltaic Generator Using Nonlinear Control

A.Yahya, H. El Fadil, Josep M. Guerrero, F. Giri, H. Erguig

Abstract— **This paper proposes a nonlinear control methodology for three phase grid connected of PV generator. It consists of a PV arrays; a voltage source inverter, a grid filter and an electric grid. The controller objectives are threefold: i) ensuring the Maximum power point tracking (MPPT) in the side of PV panels, ii) guaranteeing a power factor unit in the side of the grid, iii) ensuring the global asymptotic stability of the closed loop system. Based on the nonlinear model of the whole system, the controller is carried out using a Lyapunov approach. It is formally shown, using a theoretical stability analysis and simulation results that the proposed controller meets all the objectives.**

I. INTRODUCTION

With rising concerns about global warming and more since the last spike in oil prices that will cease to increase, renewable energy, long considered a useful adjunct course.

Today, oil and gas are still relatively cheap. With the scarcity of raw materials, the price of fossil fuels will continue to rise. At the same time that renewable energy price should decrease mainly due to technological advances and production in larger series. This is why the PV system has a great bright future in the forthcoming years. The PV grid-connected systems have become one of the most important applications of solar energy [5], [7], [8].

Different control strategy for three phase grid connected of PV modules has been largely dealt with in the specialist literature in the last few years (see e.g. [13]-[16]).

Nevertheless, good integration of medium or large PV system in the grid may therefore require additional functionality from the inverter, such as control of reactive power. Moreover, the increase in the average size of a PV system may lead to new strategies such as eliminating the DC-DC converter which is usually placed between the PV generator and inverter, and moving the MPPT to the inverter, which leads to increased simplicity, overall efficiency and a cost reduction. These two features are present in the three-phase inverter that is presented here, with the addition of a P&O MPPT algorithm.

A.Yahya is with the Faculty of Science, Ibn Tofail University, Kenitra 14000, Morocco.

H. El Fadil is with the EISEI Team, LGS Lab. ENSA, Ibn Tofail University, Kénitra, 14000, Morocco (Tel:+212 65 27 68 45; e-mail: h.elfadil@univ-ibntofail.ac.ma, corresponding author).

Josep M. Guerrero is with the Department of Energy Technology, Aalborg University, 9220 Aalborg East, Denmark (Tel: +45 2037 8262; Fax: +45 9815 1411; e-mail: joz@et.aau.dk).

F. Giri is with the GREYC Lab, UMR CNRS, University of Caen Basse-Normandie, 14032, Caen, France.

H. Erguig is with the ENSA, Ibn Tofail University, Kenitra 14000, Morocco.

The present paper is then focusing on the problem of controlling three phase grid-connected PV power generation systems. The control objectives are threefold: (i) global asymptotic stability of the whole closed-loop control system; (ii) achievement of the MPPT for the PV array; and (iii) ensuring a grid connection with unity Power Factor (PF). These objectives should be achieved in spite the climatic variables (temperature and radiation) changes. To this end, a nonlinear controller is developed using Lyapunov design technique. A theoretical analysis is developed to show that the controller actually meets its objectives a fact that is confirmed by simulation.

The paper is organized as follows: the three phase grid connected PV system is described and modeled in Section II. Section III is devoted to controller design and analysis. The controller tracking performances are illustrated by numerical simulation in Section IV.

II. SYSTEM DESCRIPTION AND MODELING

A. System description

The main circuit of three-phase grid-connected photovoltaic system is shown in Fig.1. It consists of a PV arrays; a DC link capacitor C; a three phase inverter (including six power semiconductors) that is based upon to ensure a DC-AC power conversion and unity power factor; a inductor filter L with its ESR resistance r, and an electric grid. The control inputs of the system are a PWM signals u_a, u_b and u_c taking values in the set $\{0,1\}$. The grid voltages e_{ga}, e_{gb} and e_{gc} constitute a three phase balanced system.
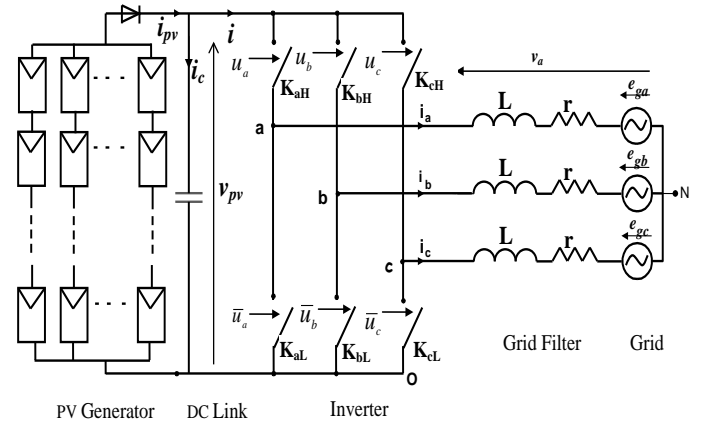

Fig.1: Three phase grid connected PV system

B. PV array model

An equivalent circuit for a PV cell is shown in Fig. 2. Its current characteristic can be found in many places (see eg. [6], [7]) and presents the following expression

$$I = I_{ph} - I_{sat}\left[\exp\left(\frac{q(V + IR_s)}{AkT}\right) - 1\right] - \frac{V + IR_s}{R_p} \qquad (1)$$

where

$$\begin{cases} I_{sat} = I_{satr}\left[\frac{T}{T_r}\right]^3 \exp\left[\frac{qE_{G0}}{Ak}\left(\frac{1}{T_r} - \frac{1}{T}\right)\right] \\ I_{ph} = \left[I_{phr} + K_I(T - 298)\right]\lambda \end{cases} \qquad (2)$$

The meaning and typical values of the parameters given by (1) and (2) can be found in many places (see e.g. [3], [4], [9]). A is diode ideal factor, k is Boltzmann constant $k = 1.38 \times 10^{-23} J/K$, T is temperature on absolute scale in K, q is electron charge $q = 1.6 \times 10^{-19} C$ and λ is the radiation in kW/m^2, I_{phr} is the short-circuit current at 298 K and 1 kW/m^2, K_I = 0.0017 A/K is the current temperature coefficient at I_{phr}, E_{G0} is the band gap for silicon, $T_r = 301.18K$ is reference temperature, I_{satr} is cell saturation current at T_r.

PV array consists of N_s cells in series formed the panel and of N_p panels in parallel according to the rated power required. The output voltage and current can be given by the following equations:

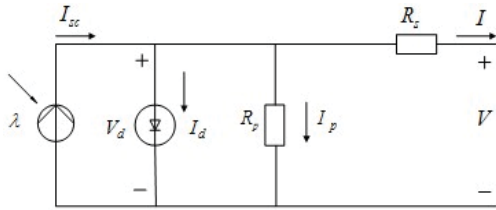$$v_{pv} = N_s(V_d - R_s I) \qquad (3)$$

$$i_{pv} = N_p I \qquad (4)$$

Fig.2 The equivalent circuit for a PV cell

The photovoltaic generator considered in this paper consists of several NU-183E1 modules. The corresponding electrical characteristics of PV modules are shown in Table I. The associated power-voltage (P-V) characteristics under changing climatic conditions (temperature and radiation) are shown in Figs. 3 and 4. This highlights the Maximum Power Point (MPP) M1 to M5, whose coordinates are given in Table III. The data in Table I to Table III will be used for simulation.

Table II shows the main characteristics of the PV array, designed using Sharp NU-183E1 modules connected in a proper series-parallel, making up a peak installed power of 71.75 kW.

As there is no DC-DC converter between the PV generator and the inverter, the PV array configuration should be chosen such that the output voltage of the photovoltaic generator is adapted to the requirements of the inverter.

In this case a 380V grid has been chosen, so the inverter would need at least 570V DC bus in order to be able to operate correctly.

The minimum number of modules connected in series should be determined by the value of the minimum DC bus voltage and the worst case climatic conditions. The PV array was found to require 28 series connected modules per string.

TABLE I: ELECTRICAL SPECIFICATIONS FOR THE SOLAR MODULE NU-183E1

Parameter	Symbol	Value
Maximum Power	Pm	183W
Short circuit current	$Iscr$	8.48A
Open circuit voltage	Voc	30.1V
Maximum power voltage	Vm	23.9V
Maximum power current	Im	7.66A
Number of parallel modules	N_p	1
Number of series modules	N_s	48

TABLE II: PV ARRAY SPECIFICATIONS USING SHARP NU-183E1

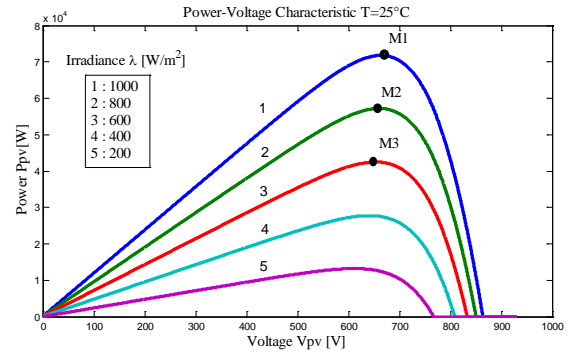| Parameter	Symbol	Value
Total peak power	P_{tm}	71.75 kW
Number of series strings	N_S	28
Number of parallel	N_P	14
Number of PV panels	N	432
Voltage in maximum power	V_m	664V
Current peak	I_m	108A

Fig.3: (P-V) characteristics of The PV Generator (N_P=14 And N_S=28) with constant temperature and varying radiation
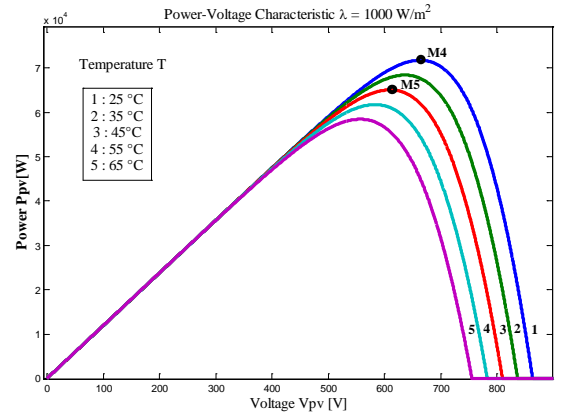

Fig.4: (P-V) characteristics of The PV Generator (N_P=14 And N_S=28) with constant radiation and varying temperature

MPP	Vm [V]	Pm [KW]
M1	664.21	71.77
M2	661.04	57.21
M3	654.34	42.50
M4	664.21	71.77
M5	610.63	65.08

C. Modeling of three-phase Grid-Connected PV System

The state-space model of a three-phase grid-connected photovoltaic system shown in Fig. 1 can be obtained by the dynamic equations described as follows:

$$\frac{d}{dt}\begin{bmatrix} i_a \\ i_b \\ i_c \end{bmatrix} = -\frac{r}{L}\begin{bmatrix} i_a \\ i_b \\ i_c \end{bmatrix} + \frac{v_{pv}}{3L}\begin{bmatrix} 2 & -1 & -1 \\ -1 & 2 & -1 \\ -1 & -1 & 2 \end{bmatrix}\begin{bmatrix} u_a \\ u_b \\ u_c \end{bmatrix} - \frac{1}{L}\begin{bmatrix} e_{ga} \\ e_{gb} \\ e_{gc} \end{bmatrix} \quad (5a)$$

$$\frac{d}{dt}v_{pv} = \frac{1}{C}i_{pv} - \frac{1}{C}\left(u_a i_a + u_b i_b + u_c i_c\right) \quad (5b)$$

Where $u_i = \begin{cases} 1 \rightarrow K_{iH} : on; \ K_{iL} : off \\ 0 \rightarrow K_{iH} : off; \ K_{iL} : on \end{cases}$

Applying the d-q transformation to (5a-b), one obtains the following instantaneous model in d-q frame

$$\frac{d}{dt}i_d = -\frac{r}{L}i_d + \omega i_q + \frac{v_{pv}}{L}u_d - \frac{1}{L}e_{gd} \quad (6a)$$

$$\frac{d}{dt}i_q = -\frac{r}{L}i_q - \omega i_d + \frac{v_{pv}}{L}u_q - \frac{1}{L}e_{gq} \quad (6b)$$

$$\frac{d}{dt}v_{pv} = -\frac{3}{2C}\left(u_d i_d + u_q i_q\right) + \frac{1}{C}i_{pv} \quad (6c)$$

Where $\left[i_{dqo}\right] = \left[T_{abc}^{dqo}\right]\left[i_{abc}\right]$; $\left[e_{gdqo}\right] = \left[T_{abc}^{dqo}\right]\left[e_{gabc}\right]$

$\left[u_{dqo}\right] = \left[T_{abc}^{dqo}\right]\left[u_{abc}\right]$

The transformation matrix T_{abc}^{dqo} is given by

$$T_{abc}^{dqo} = \frac{2}{3}\begin{bmatrix} \sin(\omega t) & \sin(\omega t - \frac{2\pi}{3}) & \sin(\omega t - \frac{4\pi}{3}) \\ \cos(\omega t) & \cos(\omega t - \frac{2\pi}{3}) & \cos(\omega t - \frac{4\pi}{3}) \\ \frac{1}{2} & \frac{1}{2} & \frac{1}{2} \end{bmatrix} \quad (7)$$

Where ω is the frequency of rotation of the reference frame in *rad/sec*. Real and reactive powers injected by the inverter can be calculated in d-q axis as follows:

$$P = \frac{3}{2}\left(e_{gd}i_d + e_{gq}i_q\right) \quad (8a)$$

$$Q = \frac{3}{2}\left(e_{gq}i_d - e_{gd}i_q\right) \quad (8b)$$

Where P is active power and Q is reactive power. In synchronous d-q rotating, $e_q = 0$, therefore

$$P = \frac{3}{2}e_{gd}i_d \quad (9a)$$

$$Q = -\frac{3}{2}e_{gd}i_q \quad (9b)$$

The active power P can be controlled by the current i_d and the reactive power Q can be controlled by the current i_q.

III. CONTROLLER DESIGN AND ANALYSIS

With the aim of design an appropriate control for the model (6) described in previous section, the control objectives, the control design and stability analysis will be investigated in this Section, taking into account the nonlinear feature and the multi-input multi-output (MIMO) aspect of the system.

A. Control objectives

In order to define the control strategy, first one has to establish the control objectives, which can be formulated as follows:
  i) Maximum power point tracking (MPPT) of PV arrays,
  ii) Unity power factor (PF) in the grid,
  iii) Asymptotic stability of the whole system.

B. Nonlinear control design

Once the control objectives are defined, as the MIMO system is highly nonlinear, a Lyapunov based nonlinear control is proposed.
The first control objective is to enforce the real power P to track the maximum power point P_M. It's already point out, that this power can be controlled by the d-axis current i_d. In this paper the MPPT algorithm based on the Perturb and Observe (P&O) technique (11) is resorted to generate the reference signal i_{dref} of the current i_d so that if $i_d = i_{dref}$ the active power P tracks its maximum value i.e. $P = P_M$.
Lets us first introduce the following error

$$e_1 = i_d - i_{dref} \quad (10)$$

In order to achieve the MPPT objective, one can seek that the error e_1 is vanishing. To this end, the dynamic of e_1 have to be clearly defined. Deriving (10), it follows from (6a) that:

$$\dot{e}_1 = -\frac{r}{L}i_d + \omega i_q + \frac{v_{pv}}{L}u_d - \frac{1}{L}e_{gd} - \dot{i}_{dref} \quad (11)$$

The goal, now, is to make e_1 exponentially vanishing by enforcing $\dot{e}_1$ to behave as follows

$$\dot{e}_1 = -c_1 e_1 \quad (12)$$

where $c_1 > 0$ being a design parameter,
Combining (11) and (12) the first control law is obtained,

$$u_d = \frac{L}{v_{pv}}\left(-c_1 e_1 + \frac{r}{L}i_d - \omega i_q + \frac{1}{L}e_{gd} + \dot{i}_{dref}\right) \quad (13)$$

The second control objective means that the grid currents i_a, i_b and i_c should be sinusoidal and in phase with the AC grid voltage e_{ga}, e_{gb} and e_{gc} respectively. To this end the reactive

power have to be null. According to (9b) the reference current i_{qref} of i_q should be zero ($i_{qref}= 0$).

The second following error is then introduced,

$$e_2 = i_q - i_{qref} \qquad (14)$$

Its derivative, using (6b), is

$$\dot{e}_2 = -\frac{r}{L}i_q - \omega\,i_d + \frac{v_{pv}}{L}u_q - \frac{1}{L}e_{gq} \qquad (15)$$

In order to achieve a power factor unit, one can seek that the error e_2 vanish exponentially. This amounts to enforcing its derivative $\dot{e}_2$ to behave as follows

$$\dot{e}_2 = -c_2 e_2 \qquad (16)$$

Where $c_2 > 0$ being a design parameter. Finally, combining (15) and (16), the second control law u_q can be easily obtained as follows

$$u_q = \frac{L}{v_{pv}}\left(-c_2 e_2 + \frac{r}{L}i_q + \omega\,i_d + \frac{1}{L}e_{gq}\right) \qquad (17)$$

Since the two control laws u_d and u_q are clearly defined, the concern now is to ensure that the stability of the closed loop is fully ensured. This will be investigated in the next Subsection.

C. Stability analysis

The objective of the global stability of closed loop system can now be analyzed. This can be carried out by checking that the proposed controllers (13) and (17) stabilize the whole system with the state vector (e_1,e_2). To this end the following quadratic Lyapunov function is considered

$$V = \frac{1}{2}e_1{}^2 + \frac{1}{2}e_2{}^2 \qquad (18)$$

Its derivative using (12) and (16) is obtained as follows

$$\dot{V} = -c_1 e_1{}^2 - c_2 e_2{}^2 \qquad (19)$$

Which means that $\dot{V} \leq 0$ and in turn shows that the equilibrium (e_1,e_2) =(0,0) of the closed loop system with state vector (e_1,e_2) is globally asymptotically stable (GAS) [12]. This also means that, for any time t_0, and whatever the initial conditions ($e_1(t_0),e_2(t_0)$), one has

$$\lim_{t\to\infty}(e_1(t),e_2(t)) \to (0,0)$$

The main results of the paper are now summarized in the following proposition.

Proposition:
Consider the closed-loop system consisting of the system of Fig.1 represented by its nonlinear model (5a-b), and the controller composed of the control laws (13) and (17). Then, one has:
   i)   The closed loop system is GAS.
   ii)   The tracking error e_1 vanishes exponentially implying MPPT achievement.
   iii) The error e_2 converges to zero implying the power factor unit.

IV. SIMULATION RESULTS

The theoretical performances of the proposed nonlinear controller are now illustrated by simulation. The

experimental setup described in Fig.5, is simulated using MATLAB/SIMULINK. The injected currents to the grid have to be synchronized with the grid voltages. To this end a phase locked loop is used as can be seen from Fig.5. The characteristics of the controlled system are listed in Table IV. Note that the controlled system is simulated using the instantaneous three phase model given by (5a-b). The model (6a-c) in d-q axis is only used in the controller design. The design parameters of the controller are given values of Table V. These parameters have been selected using a 'trial-and-error' search method and proved to be suitable. Fig.6 shows the block-diagram implementing the P&O algorithm that generates the reference current i_{dref}.

The resulting closed loop control performances are illustrated by Fig.7 to Fig.12.

TABLE IV: CHARACTERISTICS OF CONTROLLED SYSTEM

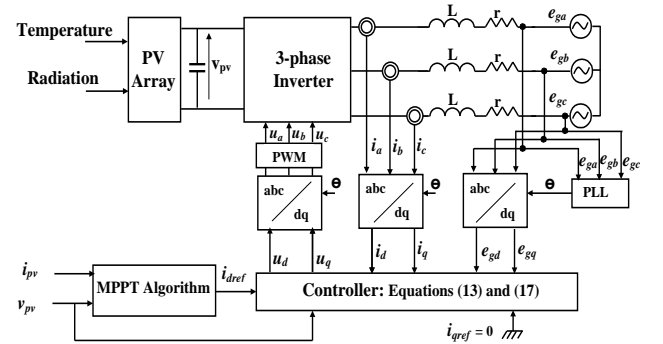| Parameter	Symbol	Value
PV array	PV power	70kW
DC link capacitor	C	3300µF
Grid filter inductor	L	3mH
	r	0.2Ω
PWM	Switching frequency	10kHz
Grid	AC source	220V
	Line frequency	50Hz

Fig.5: Simulation bench of the proposed three phase grid connected system
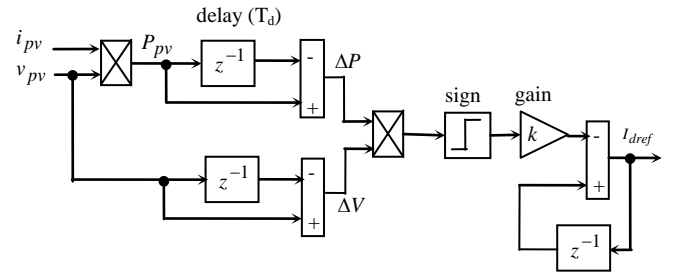

Fig.6: P&O algorithm implementation in Matlab/Simulink software

TABLE V: CONTROLLER PARAMETERS

Parameter	Symbol	Value
Design parameters	c_1	10^5
	c_2	4×10^4
P&O algorithm parameters	Delay time T_d	10^{-4}
	Step value k	0.3

A. Radiation change effect

Fig.7 shows the perfect MPPT in the presence of radiation step changes meanwhile, the temperature is kept constant, equal to 298.15K (25 °C). The simulated radiation profile is as follow: a first step change is performed between 600 and 1000W/m² at time t =0.4s and the second one between 1000 and 800W/m² at time t =0.8s. The figure shows that the PV power captured varies between (42.5kW) and (71.7kW) and then returns to (57.2kW). These values correspond (see Fig.3) to maximum points (M3, M1 and M2) of the curves associated to the considered radiation, respectively. The figure also shows that the voltage of the PV array V_{pv} varies between V_{pv} = 654.3V and V_{pv} = 664.2V and then returns to 661V, which correspond very well to the optimum voltages. Fig. 8 shows the injected currents i_a and the grid voltage e_{ga}. This figure clearly shows that the grid current i_a is sinusoidal and in phase with the grid voltage e_{ga}, proving that the power factor unit is achieved. The alternating currents injected to the grid are illustrated by Fig. 9.
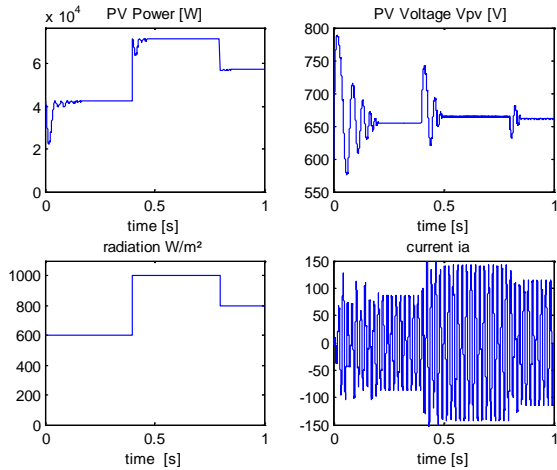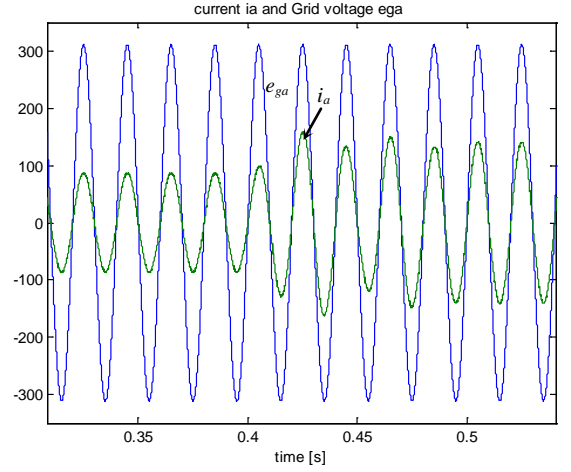

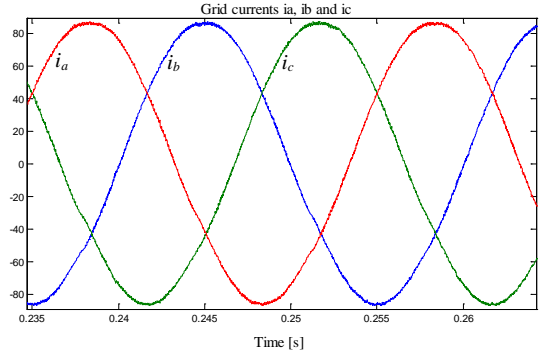Fig.8: Unity PF achievement in presence of radiation step changes

Fig.9: A zoomed waveforms of the alternating currents injected to the grid in presence of radiation step changes

B. Temperature variation effect

Fig. 10 shows the performances of the controller in presence of temperature step changes while the radiation λ is kept constant equal to 1000W/m². The temperature step change is performed at time t=0.3s between T=25°C (298.15K) and T=45°C (318.15K). It is worth noting that these changes are very abrupt which is not realistic in practical case. Nevertheless, with this important change we want to show a good robustness of the proposed controller to achieving the MPPT objective. It can be seen from Fig.10 that the system tracks the new operating point very quickly. Indeed, the captured PV power P achieves the values 71.77kW or 65kW corresponding to the maximum points (M4 and M5) associated to the temperatures 25°C and 45°C, respectively (see Fig. 4).

Fig. 11 illustrates the grid current i_a and the grid voltage e_{ga}. This figure also shows that the current i_a is sinusoidal and in phase with the voltage e_{ga} which proves the unity PF requirement.

Finally, Fig. 12 shows the zoomed three phase's grid currents and voltages.

Fig.7: MPPT capability of the controller in presence of radiation step changes.
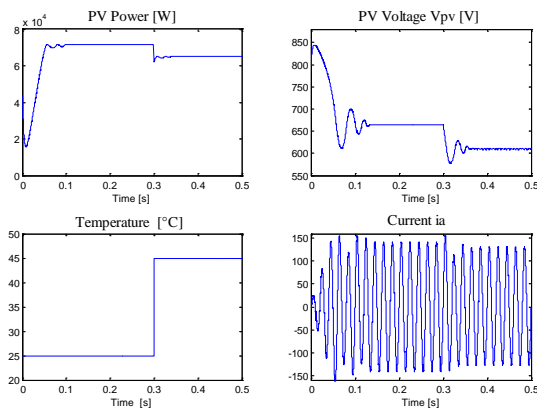
Fig.10: MPPT and DC bus voltage behavior in presence of radiation changes.
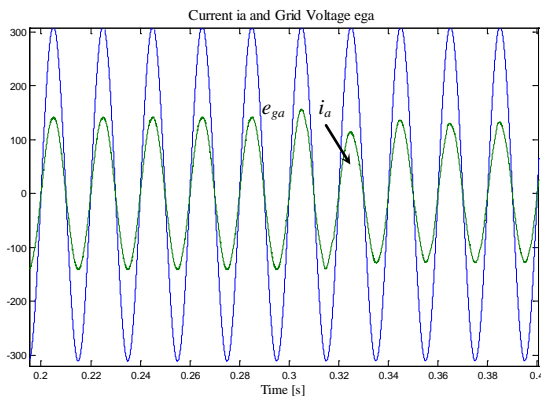

Fig.11: Unity PF behavior in presence of temperature changes
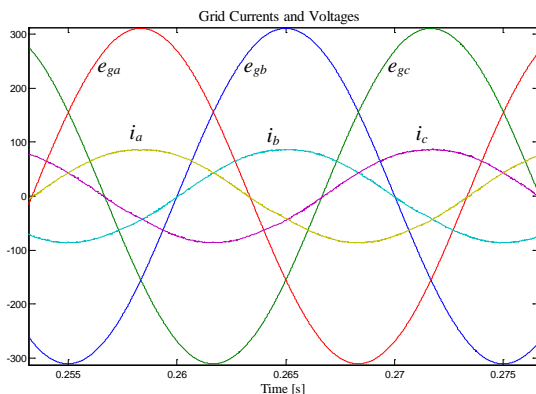

Fig. 12: Zoomed grid currents and voltages in presence of temperature step changes

V. CONCLUSION

In this paper a three phase inverter for photovoltaic applications has been presented and controlled. The main feature of the presented system is it does not require an intermediate stage of DC-DC control, as the maximum power is set by the inverter itself by means of a Perturb & Observe algorithm. The system dynamics has been described by the nonlinear state-space model (5a-b). Based on a transformed model in d-q axis, a nonlinear controller defined by (13) and (17) is designed and analyzed using a Lyapunov approach. The controller objectives are threefold: i) ensuring

the MPPT in the side of PV generator; ii) guaranteeing a power factor unit in the side of the grid, iii) ensuring the global asymptotic stability of the closed loop system. Using both formal analysis and simulation, it has been proven that the obtained controller meets all the objectives.

REFERENCES

[1] H.El Fadil , F.Giri, J.M. Guerrero. "Grid-Connected of Photovoltaic Module Using Nonlinear Control" *3rd IEEE International Symposium on Power Electronics for Distributed Generation Systems* (PEDG) 2012, pp 119-124

[2] Schonardie, Mateus F. Martins, Denizar C. ,"Three-phase grid-connected photovoltaic system with active and reactive power control using dq0 transformation," *IEEE 39th Annual Power Electronics Specialists Conference*, pp. 1202-1207, 2008.

[3] Enrique J.M., E. Duran, M. Sidrach-de-Cardona, J.M. Andujar. "Theoretical assessment of the maximum power point tracking efficiency of photovoltaic facilities with different converter topologies". *Solar Energy*, 81, pp. 31-38, 2007.

[4] Chen-Chi Chu, Chieh-Li Chen. "Robust maximum power point tracking method for photovoltaic cells: A sliding mode control approach". *Solar Energy*, 83, pp. 1370 – 1378, 2009.

[5] L. Chang and H.M. Kojabadi, "Review of interconnection standards for distributed power generation," *Large Engineering Systems Conference on Power Engineering* 2002 (LESCOPE' 02), pp.36 - 40, June 2002.

[6] Zhou dejia,Zhao Zhengming; Eltawil, Mohamed; Yuan, Liqiang ,"Design and control of a three-phase grid-connected photovoltaic system with developed maximum power point tracking," *IEEE Applied Power Electronics Conference and Exposition*, APEC, pp. 973-979, 2008.

[7] Z. Zhengming, L. Jianzheng and S. Xiaoying and Y. liqiang, *Solar Energy PV System and its Application*. Beijing: China Science Press, 2005

[8] Wu Libo,Zhao Zhengming, Liu Jianzheng , "A single-stage three-phase grid-connected photovoltaic system with modified MPPT method and reactive power compensation" *IEEE Transactions on Energy Conversion*, v 22, n4, pp. 881-886, December, 2007.

[9] El Fadil, H. and Giri, F. "Climatic sensorless maximum power point tracking in PV generation systems". *Control Engineering Practice*, Vol. 19, N.5, pp. 513 – 521, May 2011

[10] Hui Zhang, Hongwei Zhou, Jing Ren, Weizeng Liu, Shaohua Ruan and Yongjun Gao, "Three-Phase Grid-Connected Photovoltaic System with SVPWM Current Controller", *Power Electronics and Motion Control Conference*, IPEMC '09. IEEE 6th International, pp 2161-2164, 2009.

[11] Sera, D.; Mathe, L.; Kerekes, T.; Spataru, S.V.; Teodorescu, R., "On the Perturb-and-Observe and Incremental Conductance MPPT Methods for PV Systems," *Photovoltaics, IEEE Journal of* , vol.3, no.3, pp.1070-1078, July 2013

[12] Khalil H. *Nonlinear systems*. NJ, USA: Prentice Hall; 2003.

[13] Shuitao Yang; Qin Lei; Peng, F.Z.; Zhaoming Qian, "A Robust Control Scheme for Grid-Connected Voltage-Source Inverters," *Industrial Electronics, IEEE Transactions on* , vol.58, no.1, pp.202,212, Jan. 2011.

[14] Balathandayuthapani, S.; Edrington, C.S.; Henry, S.D.; Jianwu Cao, "Analysis and Control of a Photovoltaic System: Application to a High-Penetration Case Study," *Systems Journal, IEEE* , vol.6, no.2, pp.213,219, June 2012

[15] Castilla, M.; Miret, J.; Camacho, A.; Matas, J.; de Vicuna, L.G., "Reduction of Current Harmonic Distortion in Three-Phase Grid-Connected Photovoltaic Inverters via Resonant Current Control," *Industrial Electronics, IEEE Transactions on* , vol.60, no.4, pp.1464,1472, April 2013

[16] Mahmud, M.A.; Pota, H.R.; Hossain, M.J.; Roy, N.K., "Robust Partial Feedback Linearizing Stabilization Scheme for Three-Phase Grid-Connected Photovoltaic Systems," *Photovoltaics, IEEE Journal of* , vol.4, no.1, pp.423,431, Jan. 2014